doi:10.15625/2525-2518/22502



Vibrations of cracked FGM microbeams based on Modified Coupled Stress Theory

Chu Thanh Binh, Tran Van Lien*

Hanoi University of Civil Engineering, 55 Giai Phong, Hai Ba Trung, Ha Noi, Viet Nam

*Email: LienTV@huce.edu.vn

Received: 4 March 2025; Accepted for publication: 19 April 2025

Abstract. Free vibrations of cracked microbeams made of Functionally Graded Material (FGM) rested on the Winkler-Pasternak elastic foundation based on the Modified Coupled Stress Theory (MCST) are presented. Material properties of the beam vary throughout the thickness according to the power distribution and the Mori–Tanaka homogenization technique. The Timoshenko beam theory considering the size effect based on the MCST is applied. A size-dependent finite element model with new non-classical shape functions is proposed to obtain the stiffness and mass matrices of the intact FGM Timoshenko microbeam. The stiffness matrix of the cracked beam element obtained by adding an overall additional flexibility matrix to the flexibility matrix of the corresponding intact beam element can give more accurate natural frequencies. The influences of the size-effect, material, geometry, and crack parameters on natural frequencies and mode shapes are then analyzed. It is shown that the study results can be applied to other FGMs as well as more complex microbeam structures.

Keywords: crack, FGM, microbeam, MCST, nondimensional frequency.

Classification numbers: 5.4.2, 5.4.5

1. INTRODUCTION

Functionally Graded Materials (FGMs) represent a new generation of inhomogeneous composites that have garnered significant interest. Their unique thermo-mechanical properties make them versatile for various applications across industries, including aircraft, biomedical products, space vehicles, and more. Micro-Electro-Mechanical Systems (MEMS) are the new field in which FGMs have been utilized to achieve the desired performance. Micro-sized structures such as plates, sheets, beams, and framed structures are widely used in the MEMS devices, for example, electrically actuated devices, atomic force microscopes, etc.

Classical mechanical theories fail to provide satisfactory solutions for micro elements due to their inability to account for size-effects at the micro/nano scale. The Modified Couple Stress Theory (MCST) [35], which uses only one material length scale parameter to capture the size-dependent behaviour of structures and employs only the symmetric part of the couple stress tensor as a suitable measure of the continuum micro-rotation, has been chosen to analyse microstructures.

It is well known that cracks lead to a decrease in the stiffness and an increase in the flexibility of a structure. In microstructures, damages or cracks can occur due to the absence of atoms [18] or by thermal fabrication process [17]. The fundamental results of vibration analysis have been obtained more extensively for intact FGM microstructures than for cracked microstructures. The complexity of the problems in either fracture mechanics of FGMs [2, 3], as well as in the dynamics of cracked FGM microstructures with both varying material and geometry, is perhaps the major reason.

To date, there have been limited studies on the bending, vibrations and buckling of homogeneous cracked microbeams. Zhou et al. [37] analysed the dynamic characteristics of electro-statically actuated microbeams with slant cracks using the classical EBT. Utilizing the MCST combined with analytical or semi-analytical methods, Sourki and Hoseini [33] analysed free vibrations of homogeneous cracked EBT microbeams. Khorshidi and Shariati [6, 21] analysed the buckling and post-buckling of the cracked TBT microbeam. Wu et al. [34] studied the vibrational power flow of a homogeneous TBT microbeam with a crack. Atci [11] studied nonlinear vibrations of homogeneous cracked microbeams considering the longitudinal elongation effects. Shaat et al. [30] investigated the vibration of cracked nanobeams made of nanocrystalline materials based on Mindlin's couple stress theory and Mori-Tanaka model for the incorporation of the heterogeneous surface energy effects. Using FEM, Akbas [9] investigated the bending of a cracked FGM microbeam with Hermite shape functions. He analysed free vibration [8] and forced vibration of the cracked homogeneous [10] and FGM [7] cantilever under the impulse force at the free end applying the Kelvin-Voigt damping model. Kar and Srinivas [20] analysed transient responses of bi-directional FGM microbeams with edge cracks resting on nonlinear elastic foundations subjected to thermal shock loads based on the Mori-Tanaka model. Saimi et al. [28] examined the effects of cracks on the free vibrations of bidirectional FG porous microbeams in the combination with Q3D beam theory.

It is worth noting that the elastic equivalent spring model of the crack is developed based on the local flexibility matrix [12, 13, 26]. Zheng and Kessissoglou [5] demonstrated that the local flexibility matrix is especially appropriate for the analysis of a cracked beam if one employs an analytical and semi-analytical method, etc. However, the local flexibility matrix disregards the influences of shearing forces on the opening type of the crack, rendering it less accurate. The authors proposed to add an "overall additional flexibility matrix", instead of the "local additional flexibility matrix", to the flexibility matrix of the corresponding intact beam element to obtain the total flexibility matrix, and therefore the stiffness matrix. Compared with analytical results, the new stiffness matrix obtained can give more accurate natural frequencies than those resulting from using the local additional flexibility matrix.

In this work, free vibrations of FGM microbeams on a Winkler-Pasternak elastic foundation are studied based on the MCST, the TBT and the Mori–Tanaka homo-genization technique. Non-classical shape functions of the microbeam element are derived based on the governing vibration equations for the FGM microbeam using the MCST and the TBT. Using shape functions proposed, the stiffness matrix and the mass matrix of an intact microbeam are identical to the stiffness matrix and the mass matrix in the case of a homogeneous microbeam or a classical Timoshenko beam. The stiffness matrix of a cracked beam element obtained by adding an overall additional flexibility matrix to the flexibility matrix of the corresponding intact beam element can give more accurate natural frequencies. In addition, the influences of material, crack, foundation, length scale parameters and slenderness ratio on the natural frequencies of FGM microbeams are investigated in detail.

2. GOVERNING EQUATIONS OF FGM TIMOSHENKO MICROBEAMS

Consider an FGM microbeam of length L, rectangular cross-section $A = b \times h$ (Fig. 1) resting on a Winkler-Pasternak foundation. It is assumed that the material volume fraction of the FGM microbeam varies along the thickness direction as follows [31]:

$$V_{c} = \left(\frac{1}{2} + \frac{z}{h}\right)^{n}; V_{m} = 1 - \left(\frac{1}{2} + \frac{z}{h}\right)^{n}; -\frac{1}{2} \le \frac{z}{h} \le \frac{1}{2}$$
 (1)

where n is the volume fraction index, and z is the coordinates from the mid-plane of the beam. According to the Mori–Tanaka homogenization technique [25], the effective bulk modulus K and shear modulus G can be calculated by

$$\frac{K - K_m}{K_c - K_m} = \frac{V_c}{1 + (1 - V_c)(K_c - K_m) / (K_m + 4G_m / 3)}; \frac{G - G_m}{G_c - G_m} = \frac{V_c}{1 + \frac{(1 - V_c)(G_c - G_m)}{G_m + G_m (9K_m + 8G_m) / (6K_m + 12G_m)}}$$
(2)

where the subscripts m and c denote metal and ceramic materials, respectively. Effective material properties of the FGM microbeam such as Young's modulus E, Poisson's ratio v and mass density ρ can be determined as follows:

$$E(z) = \frac{9KG}{3K+G}; \ \nu(z) = \frac{3K-2G}{2(3K+G)}; \ \rho(z) = \rho_c V_c + \rho_m V_m;$$
 (3)

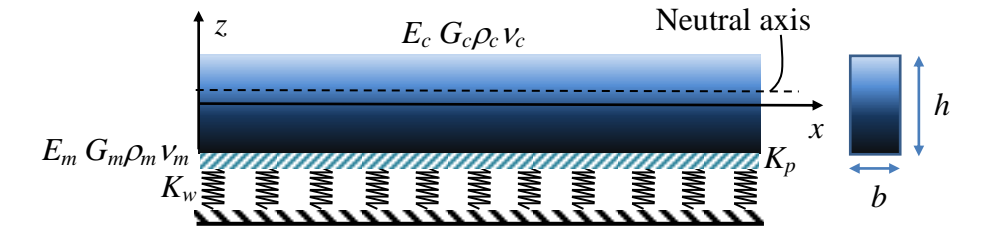


Figure 1. An FGM microbeam on a Winkler-Pasternak elastic foundation.

The displacements at a point on the cross-section of the Timoshenko beam can be represented as follows:

$$u(x,z,t) = u_0(x,t) - (z - h_0)\theta(x,t); w(x,z,t) = w_0(x,t)$$
(4)

where $u_0(x,t)$ and $w_0(x,t)$ are axial displacement and deflection of a point on the neutral axis, respectively; h_0 is the distance from the neutral axis to x-axis; $\theta(x,t)$ is the rotation angle of the cross-section. Applying the MCST, the deformation ε , stress σ , deviatoric couple stress m and curvature χ tensors can be expressed as follows:

$$\mathbf{\sigma} = 2G\mathbf{\varepsilon} + \lambda tr(\mathbf{\varepsilon})\mathbf{I}; \mathbf{\varepsilon} = \frac{1}{2} \left[\nabla \mathbf{u} + \left(\nabla \mathbf{u} \right)^T \right]; \mathbf{m} = 2G\ell^2 \chi; \chi = \frac{1}{4} \left[\nabla \left(curl \mathbf{u} \right) + \left(\nabla \left(curl \mathbf{u} \right) \right)^T \right] (5)$$

with the following nonzero components

$$\varepsilon_{xx} = \frac{\partial u_0}{\partial x} - (z - h_0) \frac{\partial \theta}{\partial x}; \quad \varepsilon_{xz} = \frac{1}{2} \left(\frac{\partial w_0}{\partial x} - \theta \right); \quad \chi_{xy} = -\frac{1}{4} \left(\frac{\partial^2 w_0}{\partial x^2} + \frac{\partial \theta}{\partial x} \right);$$

$$\sigma_{xx} = (\lambda + 2G) \varepsilon_{xx}; \quad \sigma_{xz} = 2k_s G \varepsilon_{xz}; \quad \sigma_{yy} = \sigma_{zz} = \lambda \varepsilon_{xx}; \quad m_{xy} = 2G \ell^2 \chi_{xy}$$
(6)

where λ and k_s are the Lame's coefficient and the shear correction coefficient (k_s =5/6 for a rectangular cross-section).

From Eqs. (4)-(6), the strain energy and kinetic energy variation of the microbeam based on the MCST can be obtained as follows [27]:

$$\delta U = \int_{0}^{L} \int_{A} \left(\sigma_{xx} \delta \varepsilon_{xx} + 2\sigma_{xz} \delta \varepsilon_{xz} + 2m_{xy} \delta \chi_{xy} \right) dA dx$$

$$= \int_{0}^{L} \left[N \frac{\partial \delta u_{0}}{\partial x} - M \frac{\partial \delta \theta}{\partial x} + Q \frac{\partial \delta w_{0}}{\partial x} - Q \delta \theta - \frac{1}{2} Y \frac{\partial \delta \theta}{\partial x} + \frac{1}{2} \frac{\partial Y}{\partial x} \frac{\partial \delta w_{0}}{\partial x} \right] dx - \frac{1}{2} Y \frac{\partial \delta w_{0}}{\partial x} \Big|_{0}^{L}$$

$$\delta T = \int_{0}^{L} \int_{A} \rho(z) \left\{ \left[\frac{\partial u_{0}}{\partial t} - (z - h_{0}) \frac{\partial \theta}{\partial t} \right] \left[\frac{\partial \delta u_{0}}{\partial t} - (z - h_{0}) \frac{\partial \delta \theta}{\partial t} \right] + \frac{\partial w_{0}}{\partial t} \frac{\partial \delta w_{0}}{\partial t} \right\} dA dx$$

$$= \int_{0}^{L} \left[I_{11} \left(\frac{\partial u_{0}}{\partial t} \frac{\partial \delta u_{0}}{\partial t} + \frac{\partial w_{0}}{\partial t} \frac{\partial \delta w_{0}}{\partial t} \right) - I_{12} \left(\frac{\partial u_{0}}{\partial t} \frac{\partial \delta \theta}{\partial t} + \frac{\partial \theta}{\partial t} \frac{\partial \delta u_{0}}{\partial t} \right) + I_{22} \frac{\partial \theta}{\partial t} \frac{\partial \delta \theta}{\partial t} dx$$

$$= \int_{0}^{L} \left[I_{11} \left(\frac{\partial u_{0}}{\partial t} \frac{\partial \delta u_{0}}{\partial t} + \frac{\partial w_{0}}{\partial t} \frac{\partial \delta w_{0}}{\partial t} \right) - I_{12} \left(\frac{\partial u_{0}}{\partial t} \frac{\partial \delta \theta}{\partial t} + \frac{\partial \theta}{\partial t} \frac{\partial \delta u_{0}}{\partial t} \right) + I_{22} \frac{\partial \theta}{\partial t} \frac{\partial \delta \theta}{\partial t} dx$$

where N, M, Q, and Y are the axial normal force, the bending moment, the shear force, and the couple moment, respectively:

$$N = \int_{A} \sigma_{xx} dA; Q = \int_{A} \sigma_{xz} dA; M = \int_{A} (z - h_0) \sigma_{xx} dA; Y = \int_{A} m_{xy} dA;$$
 (8)

Applying Hamilton's principle leads to the governing equations of vibration as follows:

$$A_{11} \frac{\partial^{2} u_{0}}{\partial x^{2}} - A_{12} \frac{\partial^{2} \theta}{\partial x^{2}} + p - I_{11} \frac{\partial^{2} u_{0}}{\partial t^{2}} + I_{12} \frac{\partial^{2} \theta}{\partial t^{2}} = 0$$

$$A_{12} \frac{\partial^{2} u_{0}}{\partial x^{2}} - A_{22} \frac{\partial^{2} \theta}{\partial x^{2}} - \frac{1}{4} A_{33} \ell^{2} \left(\frac{\partial^{3} w}{\partial x^{3}} + \frac{\partial^{2} \theta}{\partial x^{2}} \right) - k_{s} A_{33} \left(\frac{\partial w_{0}}{\partial x} - \theta \right) - I_{12} \frac{\partial^{2} u_{0}}{\partial t^{2}} + I_{22} \frac{\partial^{2} \theta}{\partial t^{2}} = 0$$

$$(9)$$

$$k_{s} A_{33} \left(\frac{\partial^{2} w_{0}}{\partial x^{2}} - \frac{\partial \theta}{\partial x} \right) - \frac{1}{4} A_{33} \ell^{2} \left(\frac{\partial^{4} w}{\partial x^{4}} + \frac{\partial^{3} \theta}{\partial x^{3}} \right) + q - I_{11} \frac{\partial^{2} w_{0}}{\partial t^{2}} = 0$$

where A_{11} , A_{12} , A_{22} , A_{33} are the rigidities and I_{11} , I_{12} , I_{22} are the mass moments, respectively:

$$(A_{11}, A_{12}, A_{22}) = \int_{A} \left[\lambda(z) + 2G(z) \right] \left(1, z - h_0, (z - h_0)^2 \right) dA; A_{33} = \int_{A} G(z) dA; \left(I_{11}, I_{12}, I_{22} \right) = \int_{A} \rho(z) \left(1, z - h_0, (z - h_0)^2 \right) dA$$
 (10)

where

$$h_0 = \iint_A \left[\lambda(z) + 2G(z) \right] z dA / \iint_A \left[\lambda(z) + 2G(z) \right] dA$$
 (11)

3. SHAPE FUNCTIONS OF THE FGM TIMOSHENKO MICROBEAM ELEMENT

To avoid the shear-locking problem, the solution of the equilibrium equation is adopted to interpolate the transverse displacement and rotation in derivation of the element stiffness and mass matrix. Neglecting the external static load and accepting the neutral axis, the first equation of (9) is uncoupled with the remaining equations. Thence, Eq. (9) can be rewritten as follows:

$$A_{22}\frac{d^{2}\theta}{dx^{2}} + \frac{A_{33}\ell^{2}}{4} \left(\frac{d^{3}w}{dx^{3}} + \frac{d^{2}\theta}{dx^{2}} \right) + k_{s}A_{33} \left(\frac{dw_{0}}{dx} - \theta \right) = 0; k_{s}A_{33} \left(\frac{d^{2}w_{0}}{dx^{2}} - \frac{d\theta}{dx} \right) - \frac{A_{33}\ell^{2}}{4} \left(\frac{d^{4}w}{dx^{4}} + \frac{d^{3}\theta}{dx^{3}} \right) = 0 (12)$$

Setting the new variables:

$$\gamma = \frac{dw_0}{dx} - \theta; \quad \phi = \frac{dw_0}{dx} + \theta \tag{13}$$

and integrating the second equation of (12) yield:

$$k_{s}A_{33}\gamma = \frac{A_{33}\ell^{2}}{4}\frac{d^{2}\phi}{dx^{2}} + c_{1}$$
 (14)

Using the first equation of (12) we obtain:

$$\frac{\ell^2}{8k_s} \frac{d^4 \phi}{dx^4} - \frac{1}{2} \left(1 + \frac{A_{33}\ell^2}{A_{22}} \right) \frac{d^2 \phi}{dx^2} = \frac{c_1}{A_{22}}$$
 (15)

where c_I is an integration constant. Introducing the nondimensional variable $\bar{x} = x/L$ and neglecting the first term because of $(\ell/L)^2 \approx 0$, Eq. (13) can be rewritten as follows:

$$(1+\alpha)\frac{d^2\phi}{L^2d\bar{x}^2} = -\frac{2c_1}{A_{22}} \tag{16}$$

where

$$\alpha = \frac{A_{33}\ell^2}{A_{22}} \tag{17}$$

Integrating Eq. (16) and substituting into Eq. (14) yield:

$$\phi = -\frac{c_1}{A_{22}(1+\alpha)}x^2 + c_2x + c_3; \gamma = \frac{c_1}{k_s A_{33}} \frac{1+\alpha/2}{1+\alpha}$$
(18)

and

$$\theta = \frac{1}{2} \left[-\frac{c_1}{A_{22}(1+\alpha)} x^2 + c_2 x + c_3 - \frac{c_1}{k_s A_{33}} \frac{1+\alpha/2}{1+\alpha} \right]; w_0 = \frac{1}{2} \left[-\frac{c_1}{3A_{22}(1+\alpha)} x^3 + \frac{c_2}{2} x^2 + c_3 x + \frac{c_1}{k_s A_{33}} \frac{1+\alpha/2}{1+\alpha} x \right] + c_4$$
 (19)

Using the boundary conditions

$$w_0(x=0) = w_1; \theta(x=0) = \theta_1; w_0(x=L) = w_2; \theta(x=L) = \theta_2$$
 (20)

Four integration constants c_1 , c_2 , c_3 , c_4 can be determined as follows:

$$c_{1} = \frac{A_{22}(1+\alpha)}{L^{3}(1+\varphi)} \left(-12w_{1} - 6L\theta_{1} + 12w_{2} - 6L\theta_{2}\right); c_{4} = w_{1}; c_{2} = 2\frac{\theta_{2} - \theta_{1}}{L} + \frac{c_{1}L}{A_{22}(1+\alpha)}; c_{3} = 2\theta_{1} + \frac{c_{1}L}{k_{s}A_{33}} \frac{1+\alpha/2}{(1+\alpha)} (21)$$

where φ is the ratio of the bending to the shear stiffness of the FGM microbeam element:

$$\varphi = \frac{12A_{22}}{k_s A_{33} L^2} \left(1 + \frac{\alpha}{2} \right) \tag{22}$$

φ is identical to the coefficient proposed by Kahrobaiyan *et al.* in [19] in the case of the homogeneous microbeam element. Substituting the integration constants from Eq. (21) into Eq. (19) yields the shape functions of the FGM Timoshenko microbeam element as follows:

$$N_{1}^{w} = 1 + \frac{1}{1+\varphi} \left[2\left(\frac{x}{L}\right)^{3} - 3\left(\frac{x}{L}\right)^{2} - \varphi\left(\frac{x}{L}\right) \right]; N_{2}^{w} = \frac{L}{2(1+\varphi)} \left[2\left(\frac{x}{L}\right)^{3} - (4+\varphi)\left(\frac{x}{L}\right)^{2} + (2+\varphi)\left(\frac{x}{L}\right) \right];$$

$$N_{3}^{w} = \frac{-1}{1+\varphi} \left[2\left(\frac{x}{L}\right)^{3} - 3\left(\frac{x}{L}\right)^{2} - \varphi\left(\frac{x}{L}\right) \right]; N_{4}^{w} = \frac{L}{2(1+\varphi)} \left[2\left(\frac{x}{L}\right)^{3} + (\varphi - 2)\left(\frac{x}{L}\right)^{2} - \varphi\left(\frac{x}{L}\right) \right];$$

$$N_{1}^{\theta} = -\frac{6}{L(1+\varphi)} \left(\frac{x}{L}\right) \left(1 - \frac{x}{L}\right); N_{2}^{\theta} = \left(1 - \frac{x}{L}\right) \left[1 - \frac{3}{(1+\varphi)}\left(\frac{x}{L}\right) \right];$$

$$N_{3}^{\theta} = \frac{6}{L(1+\varphi)} \left(\frac{x}{L}\right) \left(1 - \frac{x}{L}\right); N_{4}^{\theta} = \left(\frac{x}{L}\right) \left[1 - \frac{3}{(1+\varphi)}\left(1 - \frac{x}{L}\right) \right];$$

$$(23)$$

These non-classical shape functions are identical to shape functions proposed by [14-16, 19, 36] for the homogeneous Timoshenko microbeam element in the case of $A_{22} = EI$; $A_{33} = GA$. Letting $\ell = 0$ yields the shape functions of the classical Timoshenko beam element [22]. Letting $\varphi = 0$ yields the Hermite shape functions and its derivative.

4. STIFFNESS AND MASS MATRIX OF AN INTACT FGM MICROBEAM ELEMENT

The microbeam is divided into several two-node beam elements with the nodal displacements $\mathbf{d} = \left\{u_i, w_i, \theta_i, u_j, w_j, \theta_j\right\}^T$ where i and j denote the left and right nodes, respectively. The displacements and rotation angles of the FGM Timoshenko microbeam element can be interpolated as follows:

$$\begin{cases}
 u_0 \\
 w_0 \\
 \theta
\end{cases} = \begin{bmatrix}
 N_1^u & 0 & 0 & N_2^u & 0 & 0 \\
 0 & N_1^w & N_2^w & 0 & N_3^w & N_4^w \\
 0 & N_1^\theta & N_2^\theta & 0 & N_3^\theta & N_4^\theta
\end{bmatrix} \left\{ u_i \quad w_i \quad \theta_i \quad u_j \quad w_j \quad \theta_j \right\}^T = \begin{bmatrix}
 \mathbf{N}^{\mathbf{u}} \\
 \mathbf{N}^{\mathbf{w}} \\
 \mathbf{N}^{\mathbf{\theta}}
\end{bmatrix} . \mathbf{d} \tag{24}$$

where N_1^u ; N_2^u are Lagrange's shape functions of the axial displacement:

$$N_1^u = 1 - \frac{x}{L}; N_2^u = \frac{x}{L} \tag{25}$$

Using the shape functions (24) and applying the well-known procedures of FEM [38], we obtain the stiffness and the mass matrices of the intact FGM Timoshenko microbeam element based on the MCST rested on the Winkler-Pasternak elastic foundation as follows:

$$\mathbf{K}_{\mathbf{b}} = \int_{0}^{L} \left\{ A_{11} \left(\frac{\partial \mathbf{N}^{\mathbf{u}}}{\partial x} \right)^{T} \frac{\partial \mathbf{N}^{\mathbf{u}}}{\partial x} - A_{12} \left[\left(\frac{\partial \mathbf{N}^{\mathbf{u}}}{\partial x} \right)^{T} \frac{\partial \mathbf{N}^{\mathbf{\theta}}}{\partial x} + \left(\frac{\partial \mathbf{N}^{\mathbf{\theta}}}{\partial x} \right)^{T} \frac{\partial \mathbf{N}^{\mathbf{u}}}{\partial x} \right] + A_{22} \left(\frac{\partial \mathbf{N}^{\mathbf{\theta}}}{\partial x} \right)^{T} \frac{\partial \mathbf{N}^{\mathbf{\theta}}}{\partial x} \right\} dx;$$

$$\left\{ + k_{s} A_{33} \left(\frac{\partial \mathbf{N}^{\mathbf{w}}}{\partial x} - \mathbf{N}^{\mathbf{\theta}} \right)^{T} \left(\frac{\partial \mathbf{N}^{\mathbf{w}}}{\partial x} - \mathbf{N}^{\mathbf{\theta}} \right) + \frac{A_{33} \ell^{2}}{4} \left(\frac{\partial^{2} \mathbf{N}^{\mathbf{w}}}{\partial x^{2}} + \frac{\partial \mathbf{N}^{\mathbf{\theta}}}{\partial x} \right)^{T} \left(\frac{\partial^{2} \mathbf{N}^{\mathbf{w}}}{\partial x^{2}} + \frac{\partial \mathbf{N}^{\mathbf{\theta}}}{\partial x} \right) \right\} dx;$$

$$\mathbf{K}_{\mathbf{w}} = \int_{0}^{L} K_{w} \left(\mathbf{N}^{\mathbf{w}} \right)^{T} \mathbf{N}^{\mathbf{w}} dx; \quad \mathbf{K}_{\mathbf{p}} = \int_{0}^{L} K_{p} \left(\frac{\partial \mathbf{N}^{\mathbf{w}}}{\partial x} \right)^{T} \frac{\partial \mathbf{N}^{\mathbf{w}}}{\partial x} dx;$$

$$\mathbf{M} = \int_{0}^{L} \left\{ I_{11} \left[\left(\mathbf{N}^{\mathbf{u}} \right)^{T} \mathbf{N}^{\mathbf{u}} + \left(\mathbf{N}^{\mathbf{w}} \right)^{T} \mathbf{N}^{\mathbf{w}} \right] - I_{12} \left[\left(\mathbf{N}^{\mathbf{u}} \right)^{T} \mathbf{N}^{\mathbf{\theta}} + \left(\mathbf{N}^{\mathbf{\theta}} \right)^{T} \mathbf{N}^{\mathbf{u}} \right] + I_{22} \left(\mathbf{N}^{\mathbf{\theta}} \right)^{T} \mathbf{N}^{\mathbf{\theta}} \right\} dx;$$

$$(26)$$

where K_w , K_p are the Winkler-Pasternak elastic foundation coefficients. The stiffness matrix of the microbeam element can be rewritten as follows:

$$\mathbf{K}_{\mathbf{e}} = \mathbf{K}_{\mathbf{h}} + \mathbf{K}_{\mathbf{w}} + \mathbf{K}_{\mathbf{n}} \tag{27}$$

The stiffness matrix (27) is identical to the stiffness matrix proposed by Dehrouyeh-Semnani and Bahrami [14] in the case of the homogeneous microbeam element. Letting $\ell=0$ yields the stiffness matrix of the classical Timoshenko beam element [22]. Letting $\varphi = 0$ yields the stiffness matrices of the classical beam element rested on the Winkler-Pasternak foundation. The mass matrix of the microbeam (26) is identical to the mass matrix proposed by [15, 19] for the homogeneous Timoshenko microbeam in the case of $A_{22} = EI$; $A_{33} = GA$. Letting $\ell = 0$ yields the mass matrix of the classical Timoshenko beam element [22].

5. STIFFNESS MATRIX OF A CRACKED MICROBEAM ELEMENT

Figure 2 shows a cracked microbeam element under the local coordinate. The relationship between the nodal displacements (u, v, θ) and forces (U, V, Θ) can be expressed as [5].

$$\begin{cases}
 u_{j} - u_{i} \\
 v_{j} - v_{i} - L\theta_{i} \\
 \theta_{j} - \theta_{i}
\end{cases} = \mathbf{C}_{\text{total}} \begin{cases}
 U_{j} \\
 V_{j} \\
 \Theta_{j}
\end{cases} = \begin{bmatrix}
 L/A_{11} + c_{11} & -c_{12} & -c_{13} \\
 -c_{21} & L^{3}/3A_{22} + c_{22} & L^{2}/2A_{22} + c_{23} \\
 -c_{31} & L^{2}/2A_{22} + c_{32} & L/A_{22} + c_{33}
\end{bmatrix} \begin{cases}
 U_{j} \\
 V_{j} \\
 \Theta_{j}
\end{cases} (28)$$

For each list the total flexibility matrix and
$$c_{11} = \frac{2\pi}{b} \int_{0}^{a/h} \frac{1 - \mu^{2}}{E} x F_{1}^{2}(x) dx; c_{13} = \frac{12\pi}{bh} \int_{0}^{a/h} \frac{1 - \mu^{2}}{E} x F_{1}(x) F_{2}(x) dx; c_{12} = c_{13} l_{c}; c_{23} = c_{33} l_{c}$$

$$c_{22} = \frac{2\pi}{b} \left[\frac{36 l_{c}^{2}}{h^{2}} \int_{0}^{a/h} \frac{1 - \mu^{2}}{E} x F_{2}^{2}(x) dx + \int_{0}^{a/h} \frac{1 - \mu^{2}}{E} x F_{1}^{2}(x) dx \right]; c_{33} = \frac{72\pi}{bh^{2}} \int_{0}^{a/h} \frac{1 - \mu^{2}}{E} x F_{2}^{2}(x) dx$$

$$(29)$$

 F_1 , F_2 , F_{II} are the correction factors for stress intensity factors:

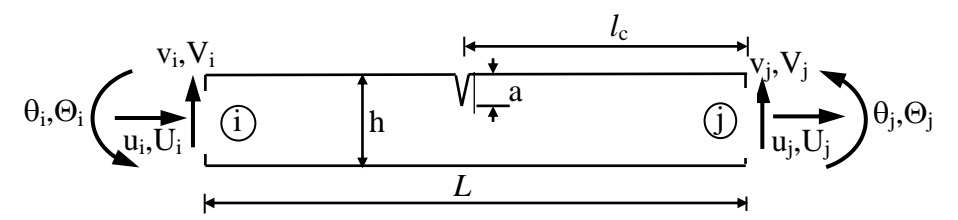


Figure 2. A cracked FGM microbeam.

$$F_{1}(s) = \sqrt{\frac{tg(\pi s/2)}{\pi s/2}} \frac{0.752 + 2.02s + 0.37(1 - \sin(\pi s/2))^{3}}{\cos(\pi s/2)}$$

$$F_{2}(s) = \sqrt{\frac{tg(\pi s/2)}{\pi s/2}} \frac{0.923 + 0.199(1 - \sin(\pi s/2))^{4}}{\cos(\pi s/2)}$$

$$F_{II}(s) = \frac{1.122 - 0.561s + 0.085s^{2} + 0.180s^{3}}{\sqrt{1 - s}}; s = \frac{a}{h}$$
(30)

The stiffness matrix \mathbf{K}_{crack} of a cracked beam element can be obtained from the total

flexibility matrix as follows [5, 29]:

$$\mathbf{K}_{\text{crack}} = \mathbf{L}\mathbf{C}_{\text{total}}^{\mathbf{1}}\mathbf{L}^{\mathbf{T}} \tag{31}$$

where

$$\mathbf{L}^{\mathbf{T}} = \begin{bmatrix} -1 & 0 & 0 & 1 & 0 & 0 \\ 0 & -1 & -L & 0 & 1 & 0 \\ 0 & 0 & -1 & 0 & 0 & 1 \end{bmatrix}$$
(32)

Finally, the discrete on FEM formulation for free vibration problems of the cracked FGM Timoshenko microbeam based on the MCST can be expressed as follows:

$$[\mathbf{M}]\{\ddot{\mathbf{D}}\} + [\mathbf{K}]\{\mathbf{D}\} = \{\mathbf{0}\}$$
(33)

where **D**, **M** and **K** are the global displacement vector, mass and stiffness matrices of the microbeam structure, respectively. Eq. (33) leads to the following characteristic equation:

$$\det\left[\mathbf{K} - \omega^2 \mathbf{M}\right] = 0 \tag{34}$$

where ω is the natural frequency of the cracked FGM Timoshenko microbeam structure.

6. NUMERICAL RESULTS AND DISCUSSION

For convenience, the non-dimensional frequencies and elastic foundation coefficients can be defined:

$$\lambda_{i} = \frac{\omega_{i} L^{2}}{h} \sqrt{\frac{\rho_{m}}{E_{m}}}; k_{w} = \frac{K_{w} L^{4}}{E_{m} I}; k_{p} = \frac{K_{p} L^{2}}{E_{m} I}; I = \frac{bh^{3}}{12}$$
(35)

The first comparison of the fundamental frequency calculated by the proposed FEM using 10 elements for the simply-supported intact FGM microbeam with those of Reddy [27], is shown in Table 1. Good agreements are also obtained for the first three nondimensional frequencies of the simply-supported intact FGM microbeam with those of Reddy.

Table 1. Comparisons of the first three frequencies of the FGM microbear	Table 1. C	omparisons of	of the	first three	frequencies	of the	FGM	microbean
--	------------	---------------	--------	-------------	-------------	--------	------------	-----------

	R	Reddy [2	Present				
n	l/h	λ_1	λ_2	λ_3	λ_1	λ_2	λ_3
0	Classical	9.83	38.82	85.63	9.8283	38.9271	86.8136
	0.2	10.65	42.06	92.78	10.6428	42.0926	93.7006
	0.4	12.80	50.52	111.34	12.7715	50.3129	111.4473
	0.6	15.73	62.01	136.39	15.6709	61.3618	134.9213
	0.8	19.08	75.05	164.51	18.9669	73.6679	160.4385
	1.0	22.66	88.84	193.82	22.4570	86.3428	188.8944
	Classical	8.67	34.29	75.59	8.6709	34.4287	77.0280
1	0.2	9.59	37.93	93.84	9.5872	38.0123	91.8873
	0.4	11.93	47.16	105.15	11.9133	47.0513	104.5548

	0.6	15.04	59.35	130.77	14.9892	58.8449	129.7974
	0.8	18.52	72.91	160.69	18.4185	71.7242	156.6851
	1.0	22.28	87.42	190.99	22.0072	84.8308	188.1667
	Classical	10.28	40.47	88.80	10.2914	40.7171	90.6812
10	0.2	11.07	43.56	95.58	11.0708	43.7379	97.2310
	0.4	13.17	51.70	113.38	13.1274	51.6587	114.2740
	0.6	16.00	62.88	137.66	15.9584	62.4185	137.0611
	0.8	19.30	75.67	165.14	19.2007	74.4929	162.0250
	1.0	22.92	89.57	194.63	22.6500	86.9891	189.0572

Table 2 presents comparisons of the nondimensional fundamental frequency ratios between the cracked homogeneous beam and the intact one, which are calculated according to the local flexibility matrix proposed by Qian *et al.* [26] and the overall additional flexibility matrix proposed by Zheng and Kessissoglou [5], with the results published by Aydin [1] and Lien *et al.* [23], which are calculated according to the rotational spring model. The obtained numerical results show good agreement with previously announced results.

Table 2. Comparisons of the fundamental frequency ratios of the beam with a single crack.

Cantilever	x ₁ /L=0.2	x ₁ /L=0.4	x ₁ /L=0.6
Aydin	0.9906	0.9958	0.9982
Lien et al.	0.9900	0.9960	0.9980
Present (Qian et al.)	0.9930	0.9971	0.9992
Present (Zheng and Kessissoglou)	0.9902	0.9960	0.9989
Clamped-Clamped	$x_1/L=0.1$	$x_1/L=0.3$	$x_1/L=0.4$
Aydin	0.9971	0.9963	0.9943
Lien et al.	0.9970	0.9960	0.9930
Present (Qian et al.)	0.9960	0.9991	0.9966
Present (Zheng and Kessissoglou)	0.9944	0.9988	0.9953
Simple-Simple	$x_1/L=0.2$	$x_1/L=0.4$	$x_1/L=0.7$
Aydin	0.9959	0.9916	0.9985
Lien et al.	0.9950	0.9910	0.9980
Present (Qian et al.)	0.9978	0.9942	0.9956
Present (Zheng and Kessissoglou)	0.9970	0.9918	0.9939

For the case study, the free vibrations of the FGM cracked microbeam of the rectangular cross-section with b=h and length L=20h, resting on the Winkler-Pasternak elastic foundation with coefficients k_w and k_p , are studied. The constituents of the microbeam include aluminum: $E_m=70$ GPa; $\rho_m=2702$ kg/m³; $\nu_m=0.3$; and ceramic: $E_c=427$ GPa; $\rho_c=3100$ kg/m³; $\nu_c=0.17$ [32]. The material length scale parameter of FG microbeams is taken as l=15 μ m in this study. The first two frequency ratios between the non-dimensional frequencies of the cracked FGM

microbeam and the intact ones will be considered, concerning the actual neutral axis position for different cracks, size effects, materials, geometry, etc.

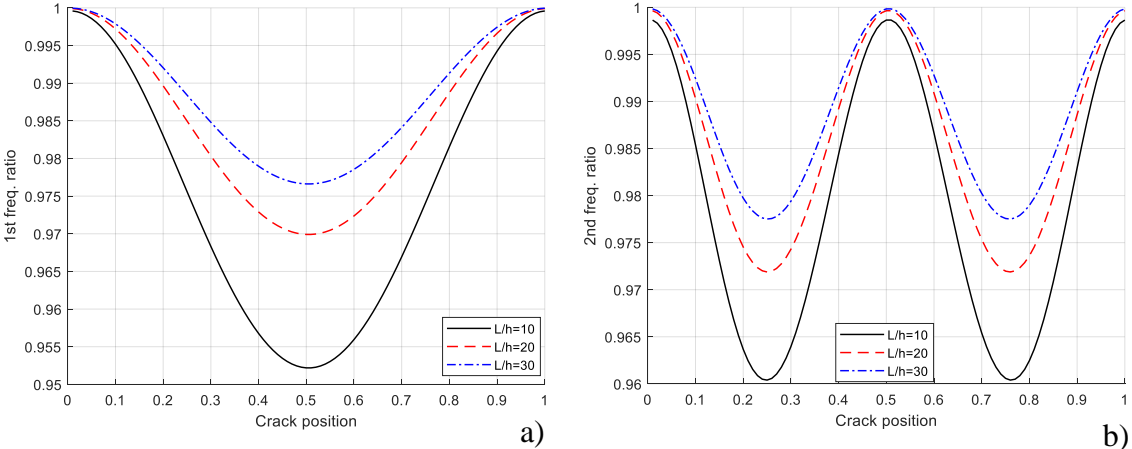


Figure 3. Changes of the first two frequency ratios of the simply supported ends microbeam considering the crack position moving along the beam length with different L/h ratios: (a) First frequency ratio, (b) Second frequency ratio.

Figure 3 shows the changes of the first two frequency ratios of the simply supported ends microbeam considering the crack position moving along the beam length with different L/h ratios: L/h = 10 (black, solid line), L/h = 20 (red, dashed line), and L/h = 30 (blue, dash-dot line). The height of the microbeam is equal to h = 30 µm, so the ratio of the material length scale parameter to the height is equal to 0.5 (l/h = 0.5). The depth of the crack is equal to 20 % of the height of the beam (a/h = 0.2), and the volume fraction index is equal to 3. It is shown that the non-dimensional frequencies of the cracked microbeam decrease remarkably when the length of the beam decreases and the crack is at some positions in the beam, for example, x/L = 0.5 for the first frequency ratio. The decrease of the lower frequency is more distinct than the decrease of the higher frequency. In the following studies, the length of the microbeam L = 20h will be considered in detail.

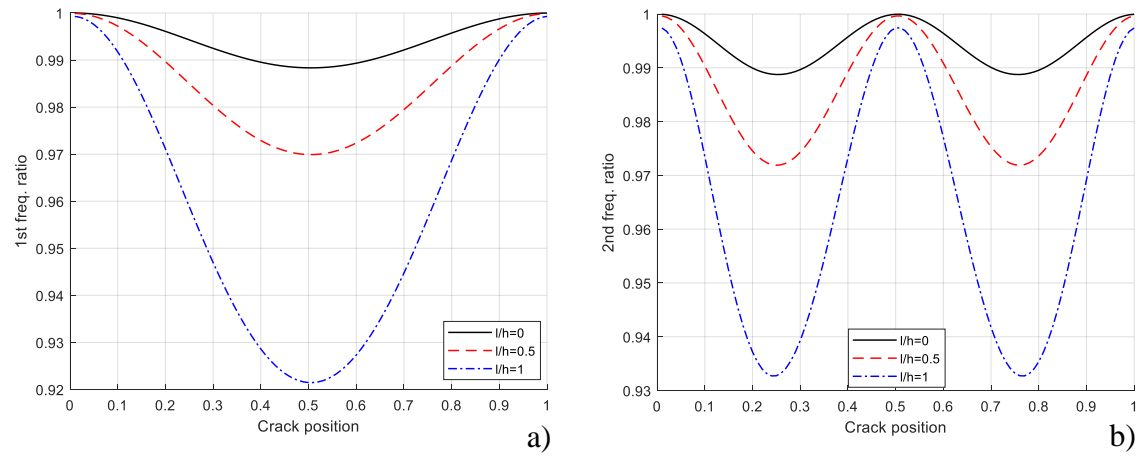


Figure 4. Changes of the first two frequency ratios of the simply supported ends microbeam considering the crack position moving along the beam length with different material length scale parameters:

(a) First frequency ratio, (b) Second frequency ratio

		Hot spot		Critical point			
Boundary condition	First frequency (x/L)	Second frequency (x/L)	Third frequency (x/L)	First frequency (x/L)	Second frequency (x/L)	Third frequency (x/L)	
Simply-supported ends	0.5;	0.25; 0.75;	0.15; 0.5; 0.85;	-	0.5;	0.33;0.66;	
Clamped ends	0; 0.50; 1;	0; 0.3; 0.7; 1;	0; 0.2; 0.5; 0.8; 1;	0.22; 0.78;	0.13; 0.5; 0.87;	0.1; 0.35; 0.65; 0.9;	
Clamped-free	0;	0; 0.54;	0; 0.31; 0.72;	-	0.22;	0.13; 0.49;	
Clamped-simply supported	0; 0.63;	0; 0.33; 0.79;	0; 0.22; 0.53; 0.86	0.26;	0.14; 0.55;	0.1; 0.38; 0.69;	

Table 3. Critical points for the first three frequencies with different boundary conditions.

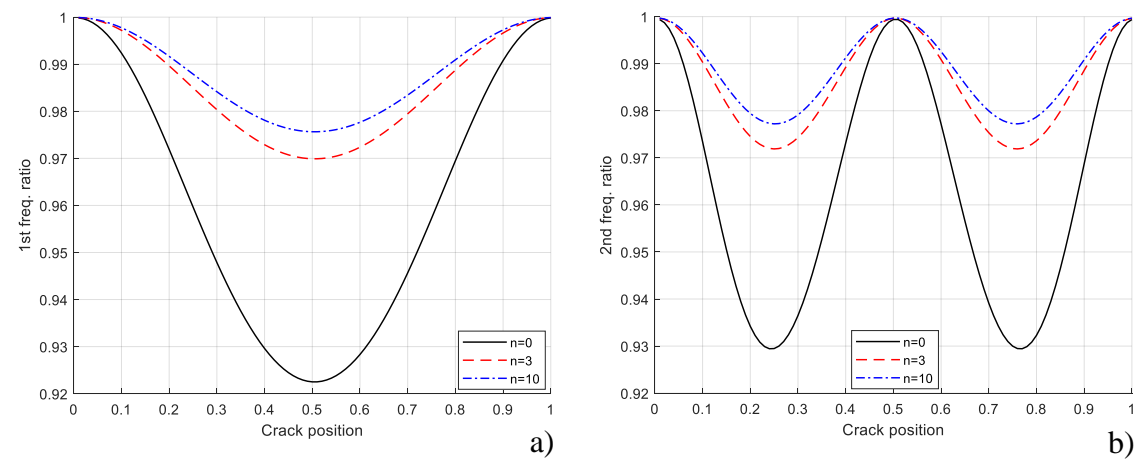
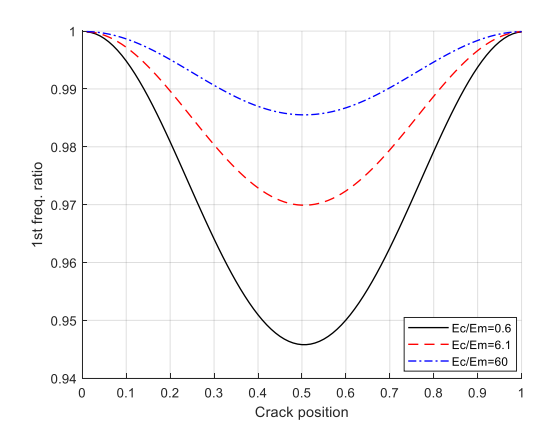


Figure 5. Changes of the first two frequency ratios of the simply supported ends microbeam considering the crack position moving along the beam length with different volume fraction indices: (a) First frequency ratio, (b) Second frequency ratio.

Figure 4 presents the changes of the first two frequency ratios of the simply supported ends microbeam considering the crack position moving along the beam length in the case of the height $h = 30 \,\mu m$ and different material length scale parameters l = 0, 15, 30 μm corresponding to l/h = 0 (black, solid line), l/h = 0.5 (red, dashed line), and l/h = 1 (blue, dash-dot line), respectively. The depth of the crack is equal to 20 % of the height of the beam (a/h = 0.2), and the volume fraction index is equal to 3. It is shown that the non-dimensional frequencies of the cracked microbeam decrease remarkably when the material length scale parameter increases and the crack is at some positions in the beam, called *hot spots* for a given frequency, such as x/L = 0.5 for the first frequency ratio, x/L = 0.25, 0.75 for the second frequency ratio, etc. Moreover, there exist positions in the beam, called *critical points* for a given frequency, at which the crack makes nondimensional frequencies unchanged or changes very little. These hot spot and critical point positions of FGM cracked microbeams coincide with the ones of homogeneous [4] and FGM macrobeams [23] or nanobeam [24] for different boundary conditions (Table 3). It is noted

that nondimensional frequencies of macrobeams or nanobeams are unchanged at critical points while nondimensional frequencies of microbeams can be unchanged or changed very little. In particular, the positions of critical points remain independent of the number of cracks. They are useful information for detecting cracks in cases where the specific frequency does not change or changes only slightly.

Figure 5 illustrates the variations in the first two frequency ratios of the microbeam as the crack position moves along the beam length. The curves represent different volume fraction indices: n = 0 (black, solid line), n = 3 (red, dashed line) and n = 10 (blue, dash-dot line). The depth of the crack is set to 20 % of the height of the beam, and the ratio of the material length scale parameter to the height of the microbeam is fixed at 0.5 (l/h = 0.5). The results indicate a significant decrease in the nondimensional frequencies of the cracked FGM microbeam as the volume fraction index decreases. In other words, the changes in nondimensional frequencies of the cracked homogeneous microbeam corresponding to n = 0 are more remarkable than the ones of FGM microbeams. The variations in frequencies of the cracked microbeam with the different volume fraction indices contrast with those observed in FGM macrobeam [23] or nanobeam [24]. Furthermore, Table 3 provides the positions of hot spots and critical points corresponding to a given frequency. The same conclusions are met in the microbeam with the other boundary conditions such as clamped ends, clamped-free and clamped-simply supported. In the following studies, the only simply supported ends microbeams are investigated for the sake of simplicity.



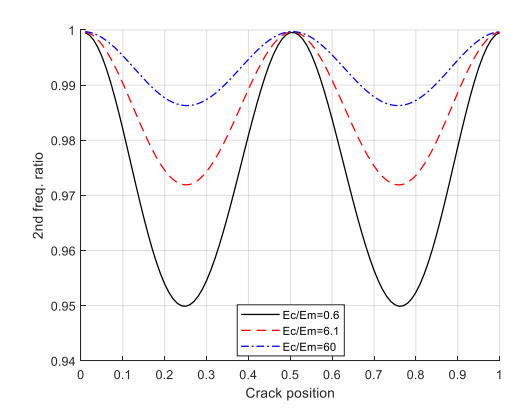


Figure 6. Changes of the first two frequency ratios of the simply supported ends microbeam considering the crack position moving along the beam length with different ratios between modulus of Young's elasticity of ceramic and metal materials: (a) First frequency ratio, (b) Second frequency ratio.

Figure 6 shows the changes of the first two frequency ratios of the microbeam considering the crack position moving along the beam length with different ratios between Young's modulus of elasticity of ceramic and metal materials: $E_c/E_m = 0.1$ (black, solid line), $E_c/E_m = 6.1$ (red, dashed line) and $E_c/E_m = 60$ (blue, dash-dot line), respectively. The depth of the crack is equal to 20 % of the height of the beam, the volume fraction index is equal to 3 and the ratio of the material length scale parameter to the height of the microbeam is equal to 0.5 (l/h = 0.5). It is shown that the non-dimensional frequencies of the cracked microbeam decrease remarkably at hot spots in the beam when the ratio between Young's modulus of elasticity of the ceramic and the metal materials decreases. The changes of frequencies of the cracked microbeam with different ratios between Young's modulus of elasticity of the ceramic and the metal materials are contrary to the ones of the FGM macrobeam [23] or the nanobeam [24].

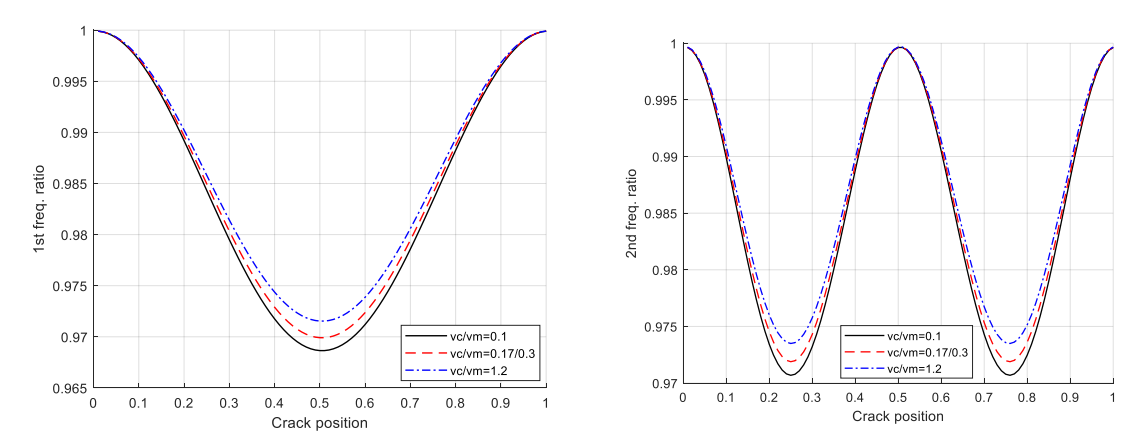


Figure 7. Changes of the first two frequency ratios of the simply supported ends microbeam considering the crack position moving along the beam length with different ratios between Poisson's coefficients of ceramic and metal materials: (a) First frequency ratio, (b) Second frequency ratio.

Figure 7 presents the changes of the first two frequency ratios of the microbeam considering the crack position moving along the beam length with different ratios between Poisson's coefficients of ceramic and metal materials: $v_c/v_m = 0.1$ (black, solid line), $v_c/v_m = 0.17/0.3$ (red, dashed line) and $v_c/v_m = 1.2$ (blue, dash-dot line). The depth of the crack is equal to 20 % of the height of the beam, the volume fraction index is equal to 3 and the ratio of the material length scale parameter to the height of the microbeam is equal to 0.5 (l/h = 0.5). It is shown that the nondimensional frequencies of the cracked microbeam decrease remarkably at hot spots in the beam when the ratio between Poisson's coefficients of the ceramic and the metal materials decreases while the influence of the change of the Poisson's coefficient on vibration frequencies at remaining positions can be ignored. It is noted that the influence of the change of Poisson's coefficient on vibration frequencies of the FGM macrobeam or nanobeam can be ignored.

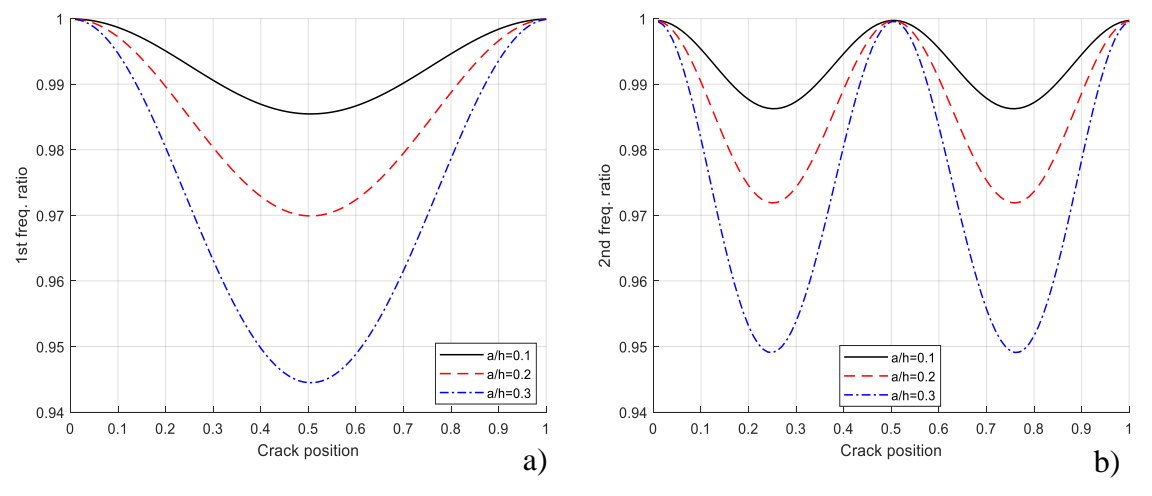


Figure 8. Changes of the first two frequency ratios of the simply supported ends microbeam considering the crack position moving along the beam length with different ratios between the crack depth and the beam height: (a) First frequency ratio, (b) Second frequency ratio.

Figure 8 illustrates the changes of the first two frequency ratios of the simply supported ends microbeam considering the crack position moving along the beam length with different ratios between the depth of the crack and the height of the beam: a/h = 0.1 (black, solid line), a/h = 0.2 (red, dashed line), and a/h = 0.3 (blue, dash-dot line). The volume fraction index is equal to 3 and the ratio of the material length scale parameter to the height of the microbeam is equal to 0.5 (l/h = 0.5). It is shown that the nondimensional frequencies of the cracked microbeam decrease remarkably when the depth of the crack increases. The changes in frequencies of the cracked FGM microbeam with different crack depths are similar to the ones of the homogeneous beam [4] and the FGM macrobeam [23] or the nanobeam [24].

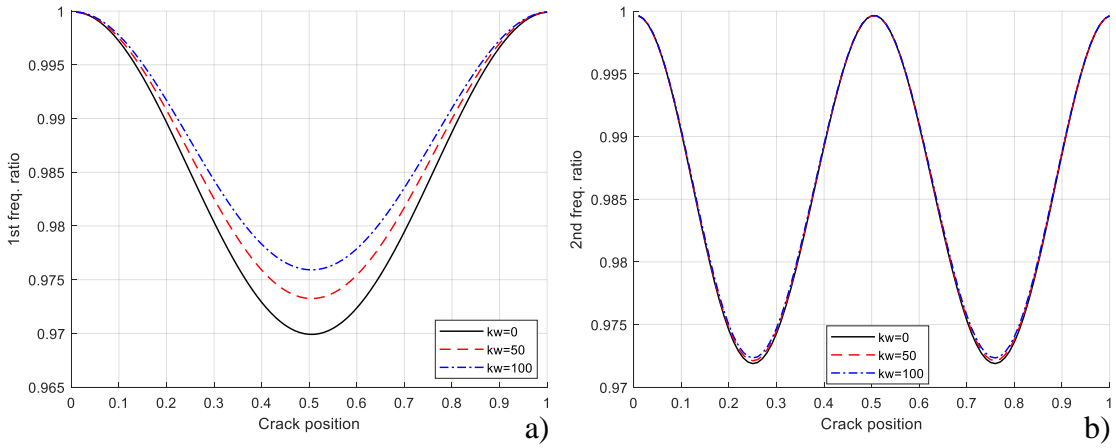


Figure 9. Changes of the first two frequency ratios of the simply supported ends microbeam considering the crack position moving along the beam length with different Winkler elastic foundation coefficients:

(a) First frequency ratio, (b) Second frequency ratio.

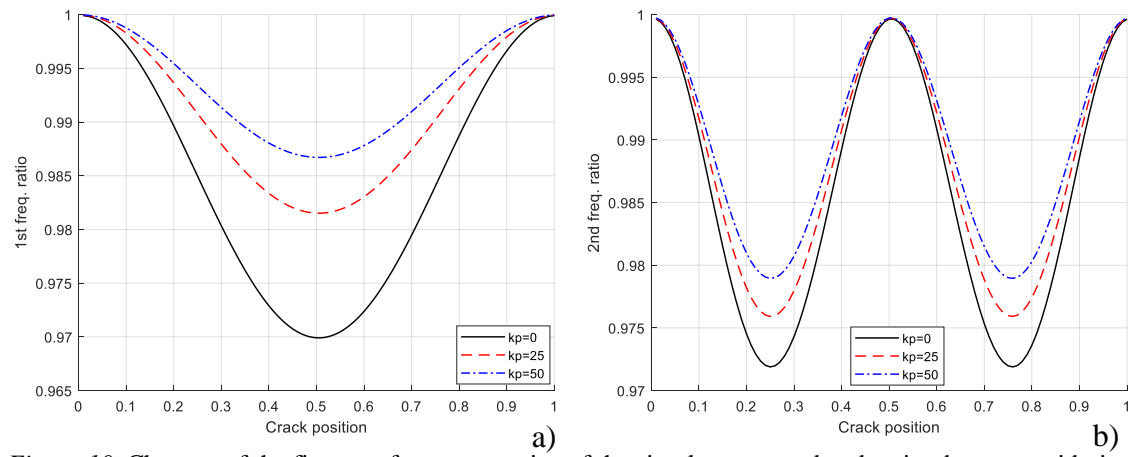


Figure 10. Changes of the first two frequency ratios of the simply supported ends microbeam considering the crack position moving along the beam length with different Pasternak's elastic foundation coefficients:

(a) First frequency ratio, (b) Second frequency ratio.

Figure 9 shows the changes of the first two frequency ratios of the simply supported ends microbeam considering the crack position moving along the beam length with different Winkler elastic foundation coefficients: k_w =0 (black, solid line), k_w =50 (red, dashed line), and k_w =100 (blue, dash-dot line). The depth of the crack is equal to 20 % of the height of the beam, the

volume fraction index is equal to 3 and the ratio of the material length scale parameter to the height of the microbeam is equal to 0.5 (l/h=0.5). It is shown that the nondimensional fundamental frequency of the cracked microbeam resting on the Winkler elastic foundation decreases remarkably when the Winkler foundation coefficient decreases. However, the influence of cracks on the higher frequencies of the FGM microbeam resting on the Winkler elastic foundation can be ignored.

Figure 10 presents the changes of the first two frequency ratios of the simply supported ends microbeam considering the crack position moving along the beam length with different Pasternak's elastic foundation coefficients: $k_p=0$ (black, solid line), $k_p=25$ (red, dashed line), and $k_p=50$ (blue, dash-dot line). The depth of the crack is equal to 20 % of the height of the beam, the volume fraction index is equal to 3 and the ratio of the material length scale parameter to the height of the microbeam is equal to 0.5 (l/h=0.5). It is shown that the non-dimensional frequencies of the cracked microbeam resting on the Pasternak elastic foundation decrease remarkably when the Pasternak foundation coefficient decreases. The changes in frequencies of the cracked microbeam with the Pasternak foundation coefficient are contrary to the ones of the FGM macrobeam or the nanobeam.

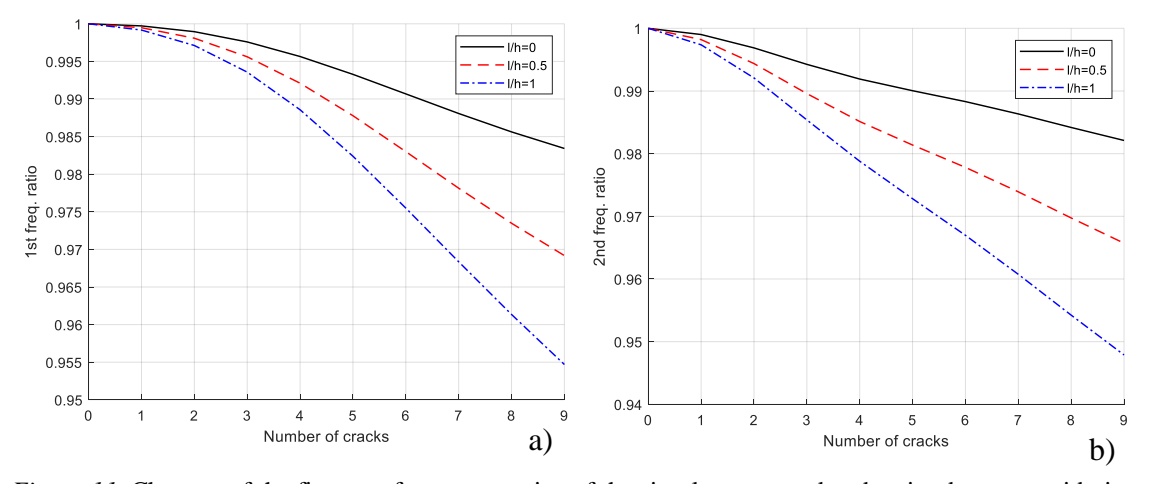


Figure 11. Changes of the first two frequency ratios of the simply supported ends microbeam considering the equidistant crack number increasing from 1 to 9 and different material length scale parameters:

(a) First frequency ratio, (b) Second frequency ratio.

Figure 11 shows the changes of the first two frequency ratios of the simply supported ends microbeam considering the equidistant crack number increasing from 1 to 9 and different material length scale parameters: l/h = 0 (black, solid line), l/h = 0.5 (red, dashed line), and l/h = 1 (blue, dash-dot line). The depth of the crack is equal to 20 % of the height of the beam, the volume fraction index is equal to 3 and the ratio of the material length scale parameter to the height of the microbeam is equal to 0.5 (l/h = 0.5). Moreover, the Winkler-Pasternak elastic foundation coefficients, k_w and k_p , are equal to 0. It is shown that the non-dimensional frequencies of the cracked FGM microbeam decrease remarkably when the number of cracks and the material length scale parameter increase.

5. CONCLUSIONS

In this paper, free vibrations of cracked FGM Timoshenko microbeams resting on the Winkler-Pasternak elastic foundation based on the MCST are presented. Material properties of

the beam vary throughout the thickness according to the power distribution and the Mori–Tanaka homogenization technique. Non-classical shape functions are proposed to obtain stiffness and mass matrices of the intact FGM Timoshenko microbeam. The stiffness matrix of the cracked beam element obtained by adding an overall additional flexibility matrix to the flexibility matrix of the corresponding intact beam element can give more accurate natural frequencies. Comparisons of the calculated results with published results are provided to validate the reliability of the proposed FEM model. Thenceforth, the influence of material length scale, geometry, materials, crack parameters and boundary conditions on the free vibration frequencies of multiple cracked FGM microbeams is studied. The calculated results show that the frequencies of the cracked FGM microbeam decrease remarkably when:

- a) The ratio of the material length scale parameter to the height of the microbeam (l/h), the ratio of the crack depth to the height of the microbeam (a/h), and the number of cracks increase.
- b) The ratio of the length to the height of the beam (L/h), the volume fraction index (n), the ratio of Young's modulus of elasticity of the ceramic and the metal (E_c/E_m) , the ratio of Poisson's coefficient of the ceramic and the metal (v_c/v_m) , and Winkler-Pasternak elastic foundation coefficients (k_w, k_p) decrease. Nevertheless, the influence of the ratio of Poisson's coefficient (v_c/v_m) and Winkler-Pasternak foundation coefficients (k_w, k_p) is not so distinct as the influence of the ratio of the length to the height of the beam (L/h), the material length scale parameter (l/h), the volume fraction index (n), the ratio of Young's modulus of elasticity of the ceramic to the metal materials (E_c/E_m) , and the depth of the crack (a/h).
- c) The decrease of lower frequencies is more obvious than higher frequencies. Moreover, the decrease in higher frequency caused by the depth of cracks is more remarkable than the ones caused by the material length scale parameter. The fundamental frequency of cracked FGM microbeams is most sensitive to the depth of the crack.
- d) The positions of hot spots and critical points in multiple cracked FGM microbeams not only align with those in homogeneous and FGM macrobeams but also remain unaffected by the material length scale parameter and the number of cracks in the beam.

All the aforementioned observations provide valuable insights for identifying cracks in multiple cracked FGM microbeams through measurements of free vibration frequencies or mode shapes. This study can be further extended to include other types of FGMs and a wider range of microstructures.

Acknowledgement. This study was funded by the Ministry of Education and Training of Viet Nam under grant number B2025.XDA.05.

Credit authorship contribution statement. Chu Thanh Binh: Data curation, Formal analysis, Investigation, Software, Validation, Investigation. Tran Van Lien: Supervision, Methodology, Funding acquisition, Review & editing

Declaration of competing interest. The authors declare that they have no known competing financial interests or personal relationships that could have appeared to influence the work reported in this paper

REFERENCES

- 1. Aydin K. Free vibration of functionally graded beams with arbitrary number of surface cracks, European Journal of Mechanics-A/Solids **42** (2013) 112-124.
- 2. Erdogan F. and Wu B. The surface crack problem for a plate with functionally graded properties, Journal of applied Mechanics **64** (3) (1997) 449-456.

- 3. Jin Z. H. and Batra R. Some basic fracture mechanics concepts in functionally graded materials, Journal of the Mechanics and Physics of Solids 44 (8) (1996) 1221-1235.
- 4. Khiem N. and Lien T. A simplified method for natural frequency analysis of a multiple cracked beam, Journal of sound and vibration **245** (4) (2001) 737-751.
- 5. Zheng D. and Kessissoglou N. Free vibration analysis of a cracked beam by finite element method, Journal of Sound and vibration **273** (3) (2004) 457-475.
- 6. Akbarzadeh Khorshidi M. and Shariati M. Buckling and postbuckling of size-dependent cracked microbeams based on a modified couple stress theory, Journal of Applied Mechanics Technical Physics **58** (2017) 717-724.
- 7. Akbas S. D. Forced vibration analysis of cracked functionally graded microbeams, Advances in Nano Research 6 (1) (2018) 39.
- 8. Akbaş Ş. D. Free vibration of edge cracked functionally graded microscale beams based on the modified couple stress theory, International Journal of Structural Stability and Dynamics **17** (03) (2017) 1750033.
- 9. Akbaş Ş. D. Bending of a cracked functionally graded nanobeam, Advances in Nano Research 6 (3) (2018) 219.
- 10. Akbaş Ş. D. Forced vibration analysis of cracked nanobeams, Journal of the Brazilian Society of Mechanical Sciences and Engineering **40** (2018) 1-11.
- 11. Atcı D. Nonlinear vibrations of cracked microbeams based on modified couple stress theory, European Journal of Mechanics A/Solids **106** (2024) 105321.
- 12. Chondros T., Dimarogonas A., and Yao J. A continuous cracked beam vibration theory. Journal of sound and vibration **215** (1) (1998) 17-34.
- 13. Chondros T., Dimarogonas A., and Yao J. Longitudinal vibration of a continuous cracked bar, Engineering Fracture Mechanics **61** (5-6) (1998) 593-606.
- 14. Dehrouyeh-Semnani A. M. and Bahrami A. On size-dependent Timoshenko beam element based on modified couple stress theory, International Journal of Engineering Science **107** (2016) 134-148.
- 15. Esen I. Dynamics of size-dependant Timoshenko micro beams subjected to moving loads, International Journal of Mechanical Sciences **175** (2020) 105501.
- 16. Esen I., Abdelrahman A. A., and Eltaher M. A. Dynamics analysis of timoshenko perforated microbeams under moving loads, Engineering with Computers **38** (3) (2022) 2413-2429.
- 17. Fang T. H. and Chang W. J. Sensitivity analysis of scanning near-field optical microscope probe, Optics & Laser Technology **35** (4) (2003) 267-271.
- 18. Ghadiri M., Soltanpour M., Yazdi A., and Safi M. Studying the influence of surface effects on vibration behavior of size-dependent cracked FG Timoshenko nanobeam considering nonlocal elasticity and elastic foundation, Applied Physics A **122** (5) (2016) 520.
- 19. Kahrobaiyan M., Asghari M., and Ahmadian M. A Timoshenko beam element based on the modified couple stress theory, International Journal of Mechanical Sciences **79** (2014) 75-83.
- 20. Kar U. K. and Srinivas J. J. E. J. O. M. A. S. Dynamic analysis and identification of bidirectional functionally graded elastically supported cracked microbeam subjected to thermal shock loads, European Journal of Mechanics-A/Solids **99** (2023) 104930.
- 21. Khorshidi M. A. and Shariati M. A multi-spring model for buckling analysis of cracked

- Timoshenko nanobeams based on modified couple stress theory, Journal of Theoretical Applied Mechanics & Materials **55** (4) (2017) 1127-1139.
- 22. Kosmatka J. An improved two-node finite element for stability and natural frequencies of axial-loaded Timoshenko beams, Computers & Structures **57** (1) (1995) 141-149.
- 23. Lien T. V., Duc N. T., and Khiem N. T. Free Vibration Analysis of Multiple Cracked Functionally Graded Timoshenko Beams, Latin American Journal of Solids and Structures **14** (9) (2017) 1752-1766.
- 24. Lien T. V., Dinh T. B., and Thang N. T. Exact closed-form solutions for the free vibration analysis of multiple cracked FGM nanobeams, Proceedings of the Institution of Mechanical Engineers, Part C: Journal of Mechanical Engineering Science **238** (8) (2024) 3373-3390.
- 25. Loja M., Barbosa J., and Soares C. M. A study on the modeling of sandwich functionally graded particulate composites, Composite Structures **94** (7) (2012) 2209-2217.
- 26. Qian G. L., Gu S. N., and Jiang J. S. The dynamic behaviour and crack detection of a beam with a crack, Journal of Sound and Vibration 138 (2) (1990) 233-243.
- 27. Reddy J. N. Microstructure-dependent couple stress theories of functionally graded beams, Journal of the Mechanics and Physics of Solids **59** (11) (2011) 2382-2399.
- 28. Saimi A., Bensaid I., and Civalek Ö. A study on the crack presence effect on dynamical behaviour of bi-directional compositionally imperfect material graded micro beams, Composite Structures **316** (2023) 117032.
- 29. Sekhar A. S. Vibration characteristics of a cracked rotor with two open cracks, Journal of Sound and Vibration **223** (4) (1999) 497-512.
- 30. Shaat M., Khorshidi M. A., Abdelkefi A., and Shariati M. Modeling and vibration characteristics of cracked nano-beams made of nanocrystalline materials, International Journal of Mechanical Sciences **115** (2016) 574-585.
- 31. Shen H. S. Functionally Graded Materials: Nonlinear Analysis Of Plates And Shells, CRC press, 2016.
- 32. Şimşek M. and Reddy J. Bending and vibration of functionally graded microbeams using a new higher order beam theory and the modified couple stress theory, International Journal of Engineering Science **64** (2013) 37-53.
- 33. Sourki R. and Hoseini S. Free vibration analysis of size-dependent cracked microbeam based on the modified couple stress theory, Applied Physics A **122** (4) (2016) 413.
- 34. Wu X. W., Zhu L. F., Wu Z. M., and Ke L. L. Vibrational power flow analysis of Timoshenko microbeams with a crack, Composite Structures **289** (2022) 115483.
- 35. Yang F., Chong A., Lam D. C. C., and Tong P. Couple stress based strain gradient theory for elasticity, International journal of solids and structures **39** (10) (2002) 2731-2743.
- 36. Zhang Q. and Liu H. On the dynamic response of porous functionally graded microbeam under moving load, International Journal of Engineering Science **153** (2020) 103317.
- 37. Zhou H., Zhang W. M., Peng Z. K., and Meng G. Dynamic Characteristics of Electrostatically Actuated Microbeams with Slant Crack, Mathematical Problems in Engineering **2015** (2015) 208065.
- 38. Zienkiewicz O. C., Taylor R. L., and Zhu J. Z. The finite element method: its basis and fundamentals, Elsevier, 2005.